NACA

RESEARCH MEMORANDUM

PERFORMANCE CHARACTERISTICS OF ONE CONVERGENT AND THREE CONVERGENT-DIVERGENT NOZZLES

By H. George Krull and Fred W. Steffen

Lewis Flight Propulsion Laboratory
Cleveland, Ohio

NATIONAL ADVISORY COMMITTEE FOR AERONAUTICS

WASHINGTON

September 29, 1952

Declassified December 1, 1959

NATIONAL ADVISORY COMMITTEE FOR AERONAUTICS

RESEARCH MEMORANDUM

PERFORMANCE CHARACTERISTICS OF ONE CONVERGENT AND THREE CONVERGENT-DIVERGENT NOZZLES

By H. George Krull and Fred W. Steffen

SUMMARY

As part of an over-all program for the experimental investigation of large-scale jet nozzles, the performance characteristics of one convergent and three convergent-divergent nozzles were obtained over a range of nozzle pressure ratios. The experimental results obtained with these nozzles were compared with one-dimensional nozzle theory.

The thrust coefficient of the convergent nozzle remained relatively high down to a nozzle pressure ratio of 0.25 (ratio of back pressure to nozzle-inlet pressure), and higher thrust coefficients were obtained with the convergent-divergent nozzles at lower nozzle pressure ratios. The convergent-divergent nozzles had low thrust coefficients when they were overexpanded, but not as low as had been predicted theoretically. The larger divergence angles seemed to increase the ratio of actual to theoretical thrust coefficient when the nozzles were overexpanded but reduced the thrust coefficient at the design pressure ratio. The loss in thrust coefficient due to skin friction for the nozzle having an expansion ratio of 2.65 was 3.7 percent, while the loss due to departure of the flow from theoretical expansion was 1 percent.

INTRODUCTION

The function of the jet nozzle of a jet-propulsion power plant is to convert the pressure energy of the gas stream into kinetic energy or thrust. It is therefore important to know the performance characteristics of jet nozzles in order to provide a basis for selecting the best nozzle for a given application and to enable the designer to predict more accurately the power-plant performance. The thrust coefficient is defined as the ratio of actual jet thrust for a nozzle of given geometry to the ideally obtainable jet thrust. With a simple convergent nozzle it has been shown theoretically and experimentally that the nozzle thrust coefficient decreases as the pressure ratio (ratio of back pressure to nozzle-inlet pressure) is decreased below critical. The fact that gains in thrust can be made by using convergent-divergent nozzles with turbojet or ram-jet engines operating at high flight Mach numbers and low nozzle pressure ratios is shown by some experimental results in reference 1. There are no known experimental data available showing the results of operating large-scale convergent-divergent nozzles at design and off-design conditions. Some small-scale data on convergent and convergent-divergent nozzles over a very limited pressure-ratio range are reported in reference 1.

In view of the fractional information available on jet nozzles, an over-all program for the experimental investigation of large-scale jet nozzles was established at the NACA Lewis laboratory. As part of this program, the performance characteristics of one convergent and three convergent-divergent nozzles were obtained and are presented herein. This investigation compares the performance characteristics of the convergent nozzle with those of the convergent-divergent nozzles over a range of nozzle pressure ratios and compares these experimental data with one-dimensional nozzle theory. The three convergent-divergent nozzles each had an exit area of about 134 square inches and were designed for expansion ratios of 1.39, 1.69, and 2.65. The convergent nozzle was operated over a pressure-ratio range from 0.78 to 0.068. The pressure-ratio range was varied from about 0.8 to at least design or lower for each of the convergent-divergent nozzles.

APPARATUS AND INSTRUMENTATION

Installation

The nozzles were installed in a test chamber connected to the laboratory combustion air and altitude exhaust facilities as shown in figures 1 and 2. The nozzles were mounted on a short section of pipe freely supported on flexure plates (fig. 2). The pipe was connected through linkage to a calibrated balanced air-pressure diaphragm for measuring thrust. A labyrinth seal around the upstream end of the short pipe separated the nozzle-inlet air from the exhaust and provided a means of maintaining a pressure difference across the nozzle.

Nozzles

The four nozzles investigated, which are shown in figure 3, included one convergent and three convergent-divergent nozzles. The convergent-divergent nozzles were designed for expansion ratios of 1.39, 1.69, and 2.65. All four nozzles, which were of simple conical construction, had inlet diameters of 21 inches and inlet half-angles of 25°. Each convergent-divergent nozzle had an over-all length of 28 inches and an exit diameter of 13 inches. Therefore, the nozzles having higher expansion ratios had smaller throats and higher divergence angles.

Instrumentation

Pressures and temperatures were measured at various stations as shown in figure 2. Ahead of the nozzle inlet at station 1 were 30 total-pressure and 14 static-pressure probes and 12 total-temperature thermocouples. Located axially along the full length of the convergent-divergent nozzle which had an expansion ratio of 2.65 were 16 wall static-pressure taps; from the throat to the exit of the other two convergent-divergent nozzles were 9 wall static taps. Static pressure at the throat of each nozzle (station 2) was measured by five trailing static-pressure tubes with two orifices each and three wall static taps. Skin thermocouples at the throat of each nozzle and ambient-exhaust-pressure instrumentation at station 0 were also provided.

PROCEDURE

Nozzle performance data were obtained over a range of pressure ratios at several different air flows. Pressure ratio was varied from a value of about 0.8 to at least design pressure ratio for the convergent-divergent nozzles and from 0.78 to 0.068 for the convergent nozzle. Early in the investigation, nozzle-wall-pressure distribution was checked for evidence of condensation shock effects. No such evidence was found. (See appendix A.)

With the size nozzles used for this investigation, it was necessary to heat the nozzle-inlet air to 450° F in order to cover the desired nozzle-pressure-ratio range with the laboratory facilities. Symbols used in this report and methods of calculation are given in appendixes B and C, respectively.

RESULTS AND DISCUSSION

One-Dimensional Flow Theory

Theoretically, a nozzle can be designed to give a thrust coefficient of unity for any nozzle pressure ratio by choosing the proper expansion ratio. A convergent-divergent nozzle theoretically has a thrust coefficient of unity at the design pressure ratio and a poor thrust coefficient when either overexpanded or underexpanded, as shown in figure 4. The theoretically calculated thrust coefficients for the convergent and the three convergent-divergent nozzles which were investigated are plotted against nozzle pressure ratio. The nozzle pressure ratio has been inverted from the conventional form in order to show more clearly the trends in the overexpanded regions of operation. For convenience, the more conventional pressure ratio has also been shown on all curves having nozzle pressure ratio as the abscissa.

An examination of the flow through and the physical forces acting on a convergent-divergent nozzle over a range of pressure ratios shows why the thrust coefficient decreases in the overexpanded and underexpanded regions of operation. The pressure distribution along the walls of a convergent-divergent nozzle over a range of pressure ratios is shown in figure 5 for constant inlet total pressure. When the exhaust pressure is sufficiently high, the flow through the nozzle is subsonic, and the nozzle, with respect to jet thrust, performs as a convergent nozzle. The flow expands subsonically in the convergent section and diffuses subsonically in the divergent section. This condition exists until the exhaust pressure is lowered sufficiently to establish exactly critical flow in the throat, as shown by curve A, figure 5. As the exhaust pressure is decreased further, the flow begins to expand supersonically in the divergent section and a normal shock moves toward the nozzle exit. The normal shock is positioned at an area ratio and Mach number where the static-pressure rise across the shock plus the subsequent subsonic diffusion in the remaining divergent section produces a jet pressure at the exit just equal to the exhaust pressure. The static-pressure distribution along the nozzle when a normal shock occurs in the divergent section is shown by curve B, figure 5. When the exhaust pressure has decreased to the point where the static-pressure rise across a normal shock at the nozzle exit design Mach number is just sufficient to raise the static pressure of the jet to the exhaust pressure, the normal shock stands at the exit of the nozzle, as noted in figure 5. Any further decrease in exhaust pressure will result in the formation of oblique shocks at the nozzle exit of such strength as to increase the static pressure of the jet to the exhaust pressure. As the exhaust pressure is decreased, the angle of inclination of the oblique shock decreases until a point is reached where no shock occurs, and the flow is then completely expanded to the exhaust pressure. The nozzle is then operating at design pressure ratio. When the exhaust pressure is higher than that which would allow the jet to expand completely, the nozzle is overexpanded. Any further decreases in the exhaust pressure below that which will allow the jet to expand completely will result in additional expansion of the flow outside the nozzle. When this condition exists, the nozzle is underexpanded.

The effects of the pressure distribution along the divergent section of the nozzle on the thrust coefficient can now be shown. For convenience, a nozzle with parallel outer walls as shown in sketch (a) will be used for this discussion.

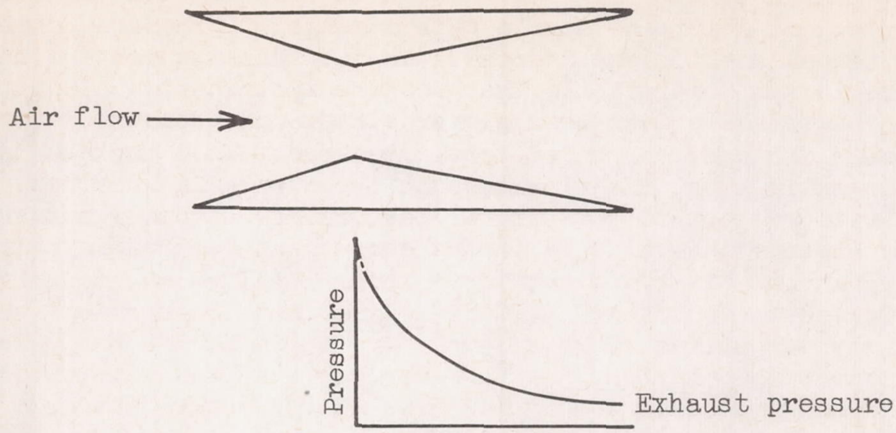

Sketch (a)

When the throat is choked, the changes in thrust will be affected only by the changes in the pressure distribution along the divergent walls. When the nozzle is operating at design pressure ratio, the pressure along the divergent wall is everywhere higher than the exhaust pressure (sketch(a)). This condition represents the maximum pressure force which can be exerted on the divergent walls; therefore the nozzle is operating at its highest efficiency.

Nozzle inefficiencies result from two possible conditions, (1) overexpansion and (2) underexpansion. To illustrate the first condition, the nozzle of sketch (a) is assumed to be overexpanded, and a normal shock stands in the divergent section of the nozzle as shown in sketch (b).

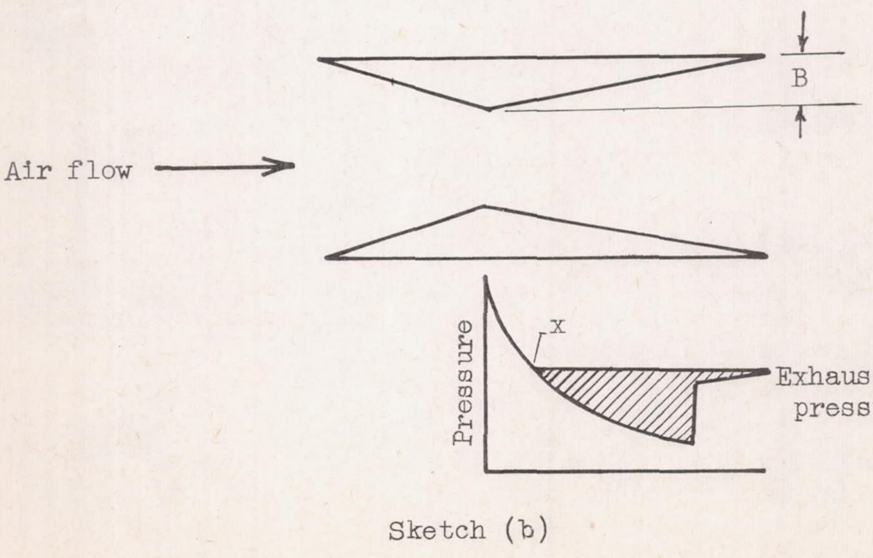

Sketch (b)

The shaded area of the pressure-distribution curve illustrates that part of the diverging section which is acted upon by pressure lower than the exhaust pressure. The nozzle is inefficient, since it could be altered to provide a higher thrust by cutting it off at the point where the wall pressure is equal to the exhaust pressure (point x, sketch (b)). The cut-off nozzle and pressure distribution for the ideal case are then shown in sketch (c).

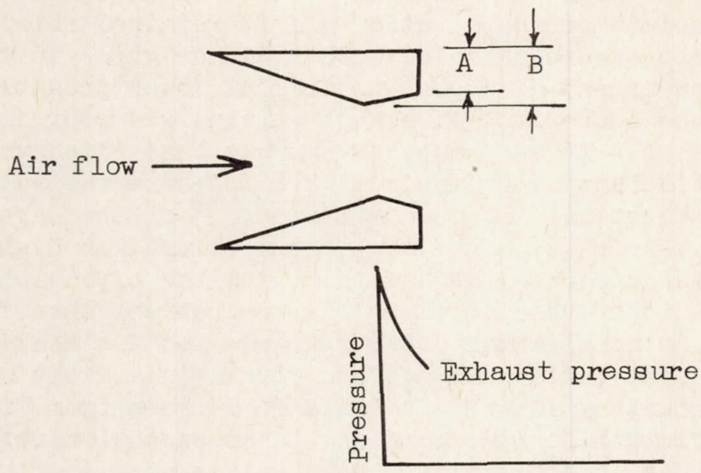

Sketch (c)

The pressure acting on the divergent wall is everywhere higher than the exhaust pressure; and if base effects are disregarded, the exhaust pressure is also acting on area A. Both nozzles have the same projected area B, but the pressure force on the cut-off nozzle is much higher than that on the nozzle in sketch (b). The cut-off nozzle would give the highest thrust which could theoretically be obtained at this nozzle pressure ratio. By comparing the pressure forces acting on the two nozzles, it can be seen why the thrust coefficient is low when a nozzle is overexpanded.

The second condition at which nozzle inefficiencies occur is a result of underexpansion. At this condition a potentially available thrust increment is lost, because an additional diverging section could be added which would be acted on by a pressure higher than exhaust pressure on the downstream face, and thus an additional positive force on the nozzle would be produced.

These inefficiencies, which have been traced to basic sources, may also be considered, thermodynamically, to be due to shock losses at various Mach numbers when the nozzle is overexpanded and to free-expansion losses when the nozzle is underexpanded.

Performance Characteristics

The experimental thrust coefficients obtained with the convergent and the three convergent-divergent nozzles are shown in figure 6 for a range of nozzle pressure ratios. The convergent-divergent nozzles had peak thrust coefficients at approximately the design pressure ratio and were 0.975, 0.955, and 0.95 for expansion ratios of 1.39, 1.69, and 2.65, respectively. The thrust coefficient of the convergent nozzle was 0.98 above critical nozzle pressure ratio, and it remained relatively high down to a nozzle pressure ratio of 0.25. Higher gains in thrust were obtained with convergent-divergent nozzles at lower pressure ratios. The performance of the convergent-divergent nozzles was poor in the overexpanded regions, but it was much better than that which was predicted from theory. This fact is shown in figure 7, where the ratio of the actual to the theoretical thrust coefficient is plotted against nozzle pressure ratio. The reason that the actual thrust was higher will be discussed in a later portion of the text. As the expansion ratio increased the ratio of the actual to the theoretical thrust coefficient increased when the nozzles were overexpanded, because the larger divergence angles allowed faster propagation of the relatively high back pressure along the boundary layer. It can also be seen from figure 6 that the thrust coefficient for the nozzle with an expansion ratio of 2.65 was actually higher at some points than for the nozzle with an expansion ratio of 1.69.

From these data it can be seen that the performance of the convergent nozzle could be calculated from one-dimensional theory within 1 or 2 percent, but that the performance of the convergent-divergent nozzles differ widely from one-dimensional theory when overexpanded and could not be foreseen because of the unpredictable behavior of the flow in the divergent section (reference 2).

The wall static pressures measured along the divergent section of the three convergent-divergent nozzles for the condition of complete expansion are compared with the wall static pressures for a theoretical isentropic expansion in figure 8. The actual pressure ratio at the throat was nearly the same for all three nozzles and was lower than critical, which means expansion was already taking place at the physical throat. Consequently, these data indicate that the flow streamlines at the throat were the same for all three nozzles and that the momentum of the gases toward the center of the flow area resulted in the formation of a vena contracta as shown in sketch (d).

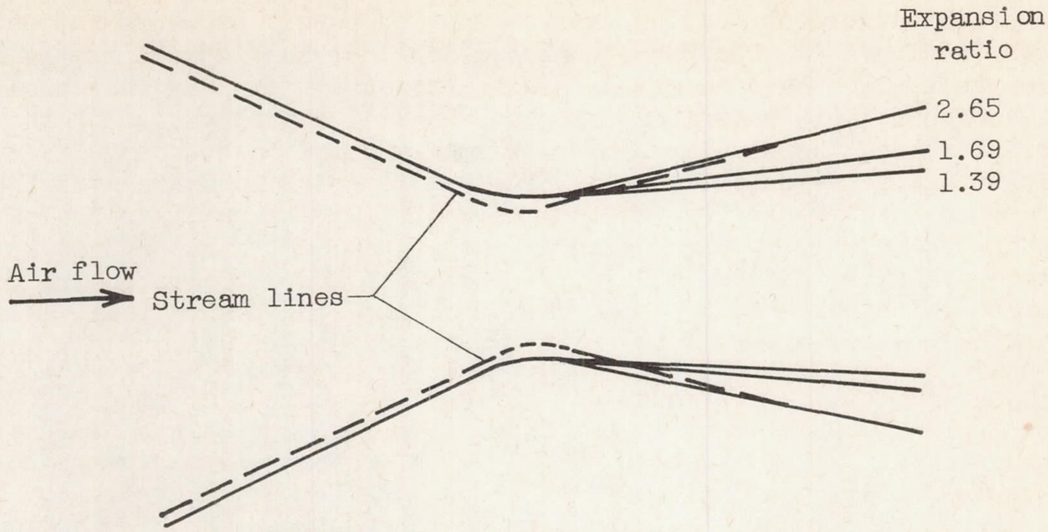

Sketch (d)

The physical throat was located in a fairly flat transition section between the convergent and the divergent portions of the nozzles (see fig. 3). Apparently then, if a vena contracta forms, the flow will have a certain amount of free expansion before coming into contact with the diverging walls of the nozzles, and the amount of free expansion will depend upon the divergence angle as shown in sketch (d). The effect of divergence angle on the expansion of the flow is indicated by the data in figure 8. The expanding flow in the nozzle with an expansion ratio of 1.39 was a series of expansions and compressions (shocks). The freely expanding flow, after the vena contracta, hit the low diverging walls, shown schematically on sketch (d), shocked (compressed), expanded, shocked, and then expanded to the exit. With the higher divergence angle of the nozzle having an expansion ratio of 1.69, more free expansion took place before the flow struck the diverging walls; and only one shock resulted, followed by expansion to the exit. The nozzle which had an expansion ratio of 2.65 and the largest divergence angle had the largest amount of free expansion. Because of the high divergence of the walls, the flow became adjacent to the wall without a large deflection in flow direction, and consequently no shock (compression) was evident from the data in figure 8.

The lower values of thrust coefficient at the design pressure ratio obtained with the nozzles with higher expansion ratios were probably due in part to the greater degree of free expansion at the beginning of the expansion process allowed by the greater wall divergence, which resulted in lower pressures acting on this portion of the diverging section of the nozzle.

A wall-pressure survey along the divergent sections of the three convergent-divergent nozzles over a range of nozzle pressure ratios is shown in figure 9. Contrary to theory, an increase in wall static pressures took place as soon as the nozzle pressure ratio was increased above the design value. This increase was caused by a propagation of the back pressure along the boundary layer, which resulted in boundary-layer thickening (references 2 and 3). The experimental pressure distribution is compared in figure 10 with the theoretical pressure distribution along the diverging wall of the nozzle with an expansion ratio of 2.65 at a nozzle pressure ratio of 0.65. The fact that the actual pressure force exerted on the divergent walls was higher than the theoretical value explains why the experimental thrust coefficient was higher than the theoretical value in the overexpanded region.

The corrected air flow per unit area for each of the four nozzles investigated is plotted against nozzle pressure ratio in figure 11. The critical air flow was maintained at higher nozzle pressure ratios for the convergent-divergent nozzles than for the convergent nozzle because of the diffuser action of the divergent section. The nozzles with expansion ratios of 1.39 and 1.69 maintained a constant air flow over the range of pressure ratios covered, which means these nozzles were always choked. However, the nozzle with an expansion ratio of 2.65 showed a decrease in air flow above a nozzle pressure ratio of 0.69, which indicated that it had unchoked. These facts are also evident from figure 9. The pressure at the throat of the two nozzles with lower expansion ratios did not change for the range of nozzle pressure ratios covered, which indicated no unchoking. The pressure at the throat of the high-expansion-ratio nozzle began to increase after a nozzle pressure ratio of 0.55 was reached, which indicated unchoking at a lower nozzle pressure ratio than for the other two nozzles. Theoretically, however, the nozzle with an expansion ratio of 2.65 should unchoke at a higher pressure ratio than the other two nozzles (fig. 4); but because of the high divergence angle, which caused faster propagation of the back pressure along the boundary layer, the nozzle unchoked sooner.

The theoretical value of the air-flow parameter for critical flow at the throat of a nozzle is 0.344. The ratio of the experimental values of air-flow parameter (fig. 11) to the theoretical value, gives a flow coefficient of 0.99 for the convergent-divergent nozzles and a flow coefficient of 0.98 for the convergent nozzle. The difference between the two could be due to the influence of the divergent-nozzle walls on the flow in the vicinity of the nozzle throat.

A breakdown of the losses occurring in the nozzle with an expansion ratio of 2.65 is shown in figure 12, where a dimensionless thrust parameter is plotted against nozzle pressure ratio. The difference between the thrust parameter calculated from one-dimensional theory and the thrust parameter calculated from an integration of wall static pressures around the complete contour of the nozzle shows the loss in thrust due to departure of the flow from theoretical expansion. At the design pressure ratio this loss amounted to 1 percent. The difference between the thrust parameter calculated from the wall static pressures and that obtained from balance-scale measurements shows the loss due to skin friction, which was 3.7 percent at design pressure ratio. Even though these nozzles were simply designed, the largest loss was due to skin friction rather than to departure of the flow from theoretical expansion. Therefore, the most important design consideration is the reduction in skin friction.

CONCLUDING REMARKS

The simple convergent nozzle can be used at nozzle pressure ratios down to 0.25 (ratio of back pressure to nozzle-inlet pressure) and still maintain a relatively high thrust coefficient. At the lower nozzle pressure ratios, higher thrust coefficients can be obtained with convergent-divergent nozzles operating at design pressure ratio. Peak thrust coefficients from 0.95 to 0.975 can be obtained with convergent-divergent nozzles having expansion ratios from 1.39 to 2.65 as compared with a peak thrust coefficient of 0.98 with a convergent nozzle. Convergent-divergent nozzles have low thrust coefficients when overexpanded, but not as low as was predicted from theory. The performance of a convergent nozzle can be calculated from one-dimensional theory within 1 or 2 percent, while the performance of a convergent-divergent nozzle differs widely from theory when overexpanded and cannot be foreseen because of the unpredictable behavior of the flow in the divergent section.

The convergent-divergent nozzles with higher divergence angles had the highest ratios of actual to theoretical thrust coefficients when the nozzles were overexpanded but the lowest thrust coefficients at the design pressure ratio. A large divergence angle also appeared to cause a nozzle to unchoke at a lower pressure ratio than expected. The convergent and convergent-divergent nozzles had flow coefficients of 0.98 and 0.99, respectively, when choked. An examination of the internal losses of the nozzle having an expansion ratio of 2.65 showed that the loss in thrust due to skin friction was 3 to 4 times the loss due to departure of the flow from theoretical expansion. Therefore, the most important design consideration is reduction in skin friction.

Lewis Flight Propulsion Laboratory
National Advisory Committee for Aeronautics
Cleveland, Ohio

APPENDIX A

CHECK FOR CONDENSATION SHOCK

Early in the investigation a check was made to see if condensation shock was present in such a form as to affect the thrust of the nozzles. The nozzle with an expansion ratio of 1.39 was investigated with wet air (33 grains water/lb) at 500° F and dry air (1.5 grains water/lb) at 90° and 500° F. A plot of the wall static pressure along the divergent section of the nozzle for each of these conditions is shown in figure 13. Since the curves all generalized, condensation shock was not present in such a form as to affect the wall pressures, and therefore the nozzle thrust was not affected. A spot check was made with the nozzle having an expansion ratio of 2.65 and no effect of condensation shock was observed.

APPENDIX B

SYMBOLS

The following symbols are used in this report:

A area, sq ft

C_T thrust coefficient

C_x thermal-expansion ratio, ratio of hot area to cold area

F thrust, lb

F_d balanced air-pressure-diaphragm reading, lb

g acceleration due to gravity, 32.2 ft/sec^2

P total pressure, lb/sq ft abs

p static pressure, lb/sq ft abs

R gas constant, 53.3 ft-lb/(lb)($^{\circ}$R) for air

T total temperature, $^{\circ}$R

V velocity, ft/sec

W_a air flow, lb/sec

γ ratio of specific heats

δ ratio of total pressure at nozzle inlet to absolute pressure at NACA standard sea-level conditions

θ ratio of total temperature at nozzle inlet to absolute temperature at NACA standard sea-level conditions.

Subscripts:

e nozzle exit

i ideal

j jet

s labyrinth seal

t	theoretical
0	exhaust
1	nozzle inlet
2	nozzle throat

APPENDIX C

METHODS OF CALCULATION

Air flow. - The nozzle air flow was computed as

$$W_a = \frac{p_2 A_2 C_x}{\sqrt{RT_1}} \sqrt{2g \frac{\gamma}{\gamma-1}\left[\left(\frac{P_1}{p_2}\right)^{\frac{\gamma-1}{\gamma}} - 1\right]\left(\frac{P_1}{p_2}\right)^{\frac{\gamma-1}{\gamma}}}$$

where γ was assumed to be 1.4. The total pressure at station 2 was assumed to be equal to that measured at station 1. Values of the thermal expansion ratio C_x of the exhaust nozzle were determined from the thermal-expansion coefficient for the exhaust-nozzle material and the measured skin temperature.

Thrust. - The jet thrust was defined as

$$F_j = M_1 V_e + A_e(p_e - p_0)$$

and the actual jet thrust was calculated by the equation

$$F_j = \frac{W_a}{g} V_1 + C_x A_s (p_1 - p_0) - F_d$$

where F_d was obtained from balanced air-pressure-diaphragm measurements. Values of the thermal-expansion ratio C_x of the pipe area under the labyrinth seal were obtained from the thermal-expansion coefficient for the pipe and the temperature of the pipe. The pipe temperature was assumed to be the same as the temperature of the air flowing through the pipe and labyrinth seal.

The ideally available jet thrust was calculated as

$$F_i = W_a \sqrt{\frac{2R}{g} \frac{\gamma}{\gamma-1} T_1 \left[1 - \left(\frac{p_0}{P_1}\right)^{\frac{\gamma-1}{\gamma}}\right]}$$

Thrust coefficient. - The thrust coefficient is defined as the ratio of the actual jet thrust to the ideally available jet thrust

$$C_T = \frac{F_j}{F_i}$$

REFERENCES

1. Schairer, G.: Performance Characteristics of Jet Nozzles. Doc. No. D-12054, Boeing Airplane Co., Seattle (Wash.), July 25, 1951.

2. Donaldson, Coleman duP.: Effects of Interaction Between Normal Shock and Boundary Layer. NACA CB 4A27, 1944.

3. Kantrowitz, Arthur, Street, Robert E., and Erwin, John R.: Study of the Two-Dimensional Flow Through a Convergent-Divergent Nozzle. NACA CB 3D24, 1943.

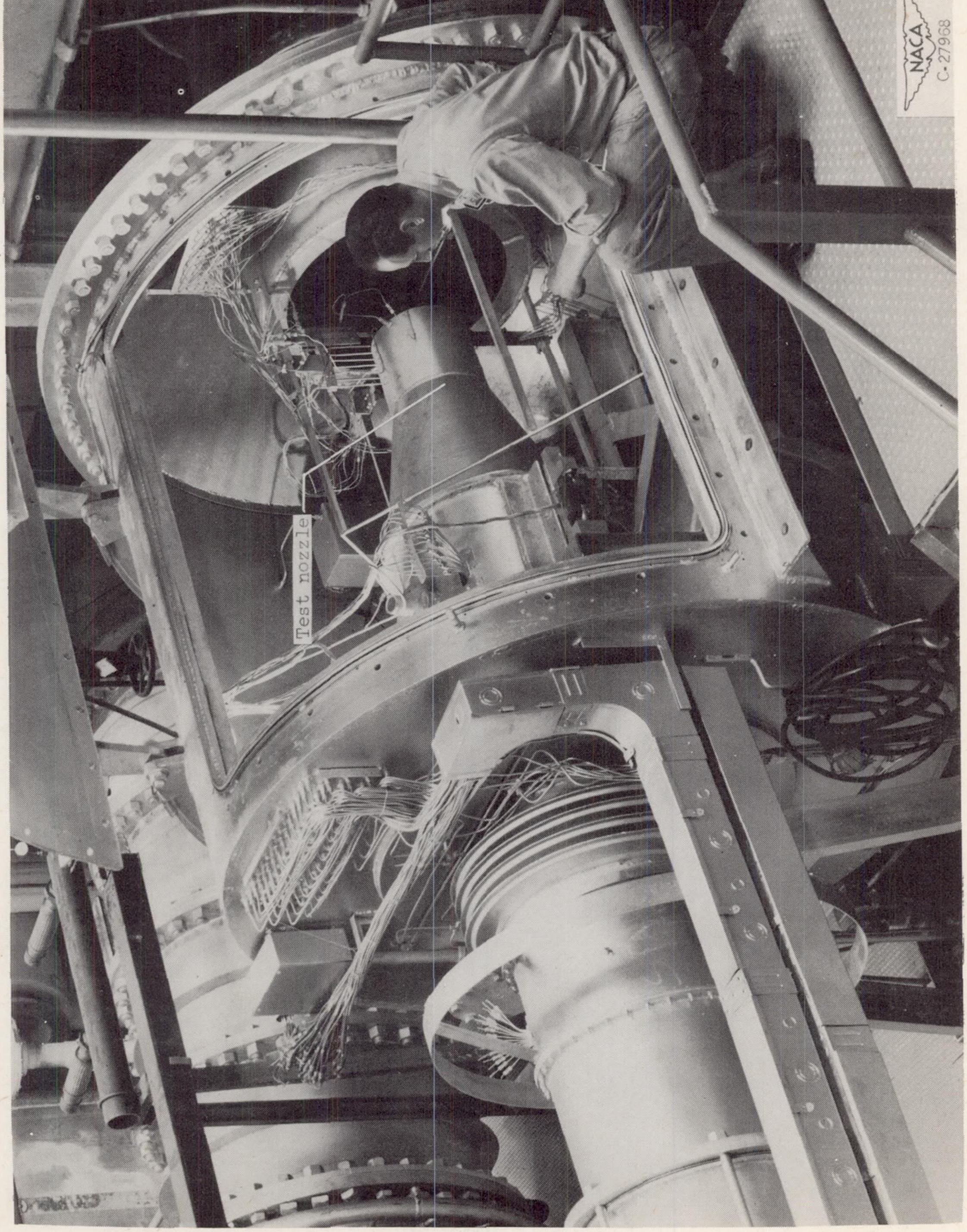

Figure 1. - Installation of nozzle in test chamber.

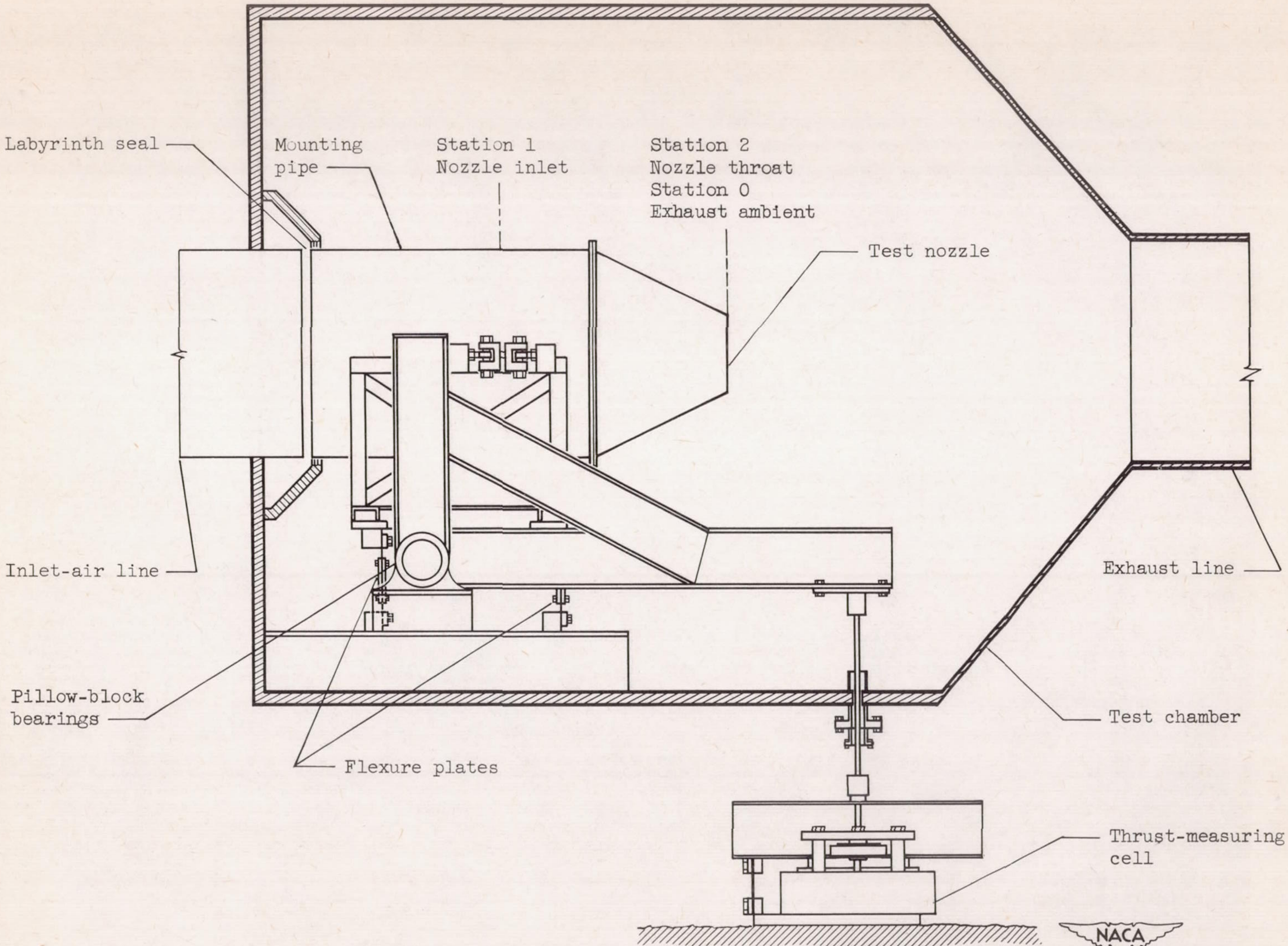

Figure 2. - Schematic drawing of nozzle in test chamber.

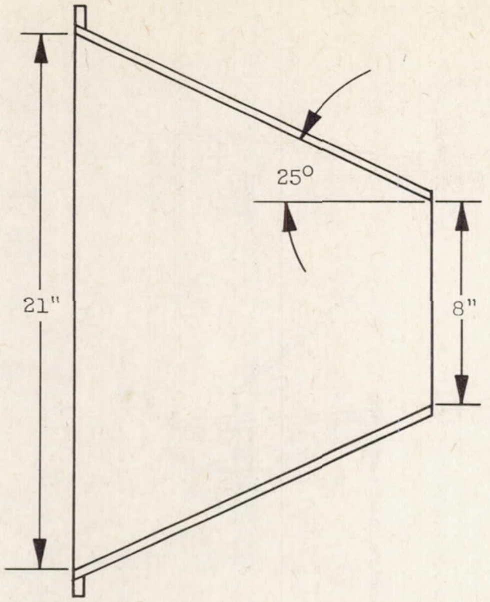

(a) Convergent nozzle.

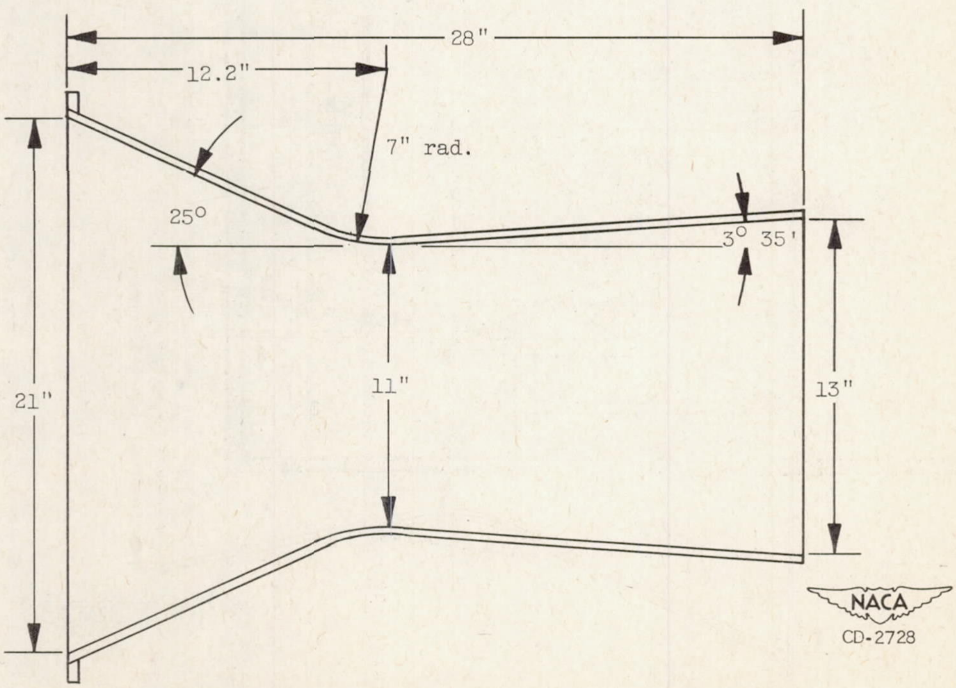

(b) Convergent-divergent nozzle, expansion ratio 1.39.

Figure 3. - Schematic diagrams of convergent and convergent-divergent nozzles.

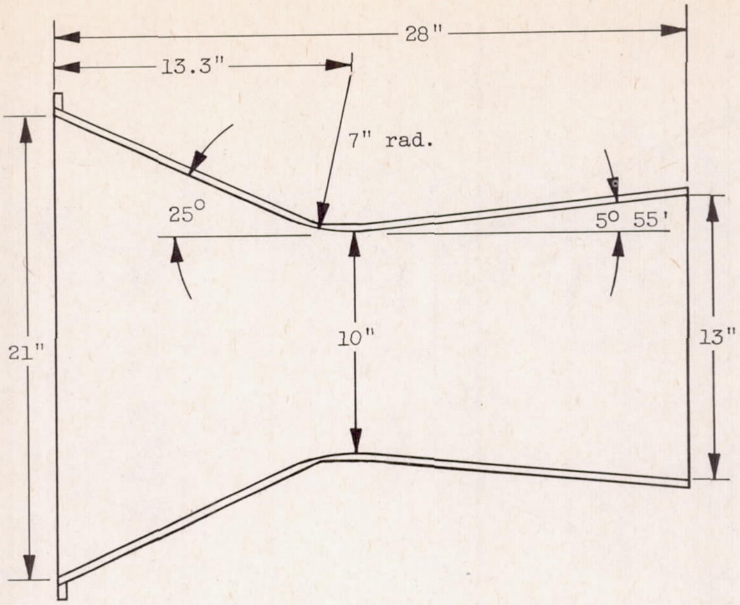

(c) Convergent-divergent nozzle, expansion ratio 1.69.

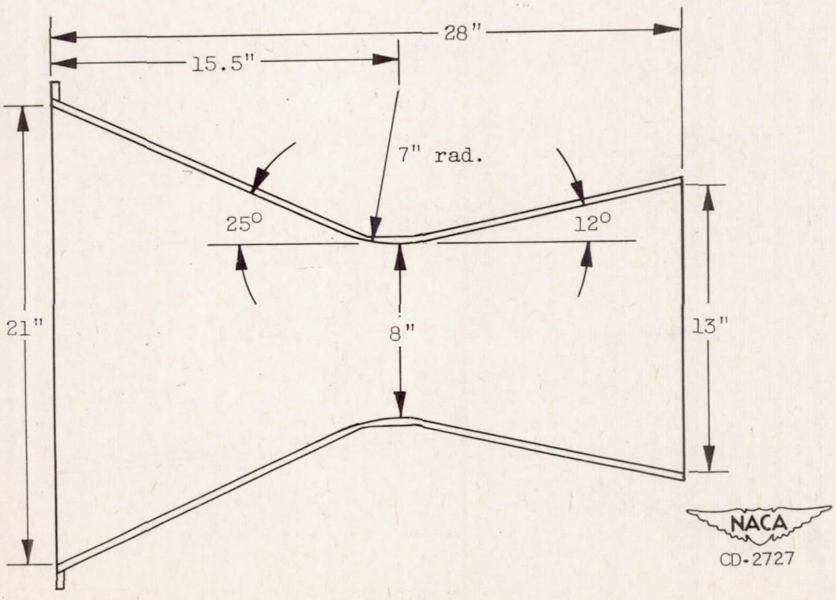

(d) Convergent-divergent nozzle, expansion ratio 2.65.

Figure 3. - Concluded. Schematic diagrams of convergent and convergent-divergent nozzles.

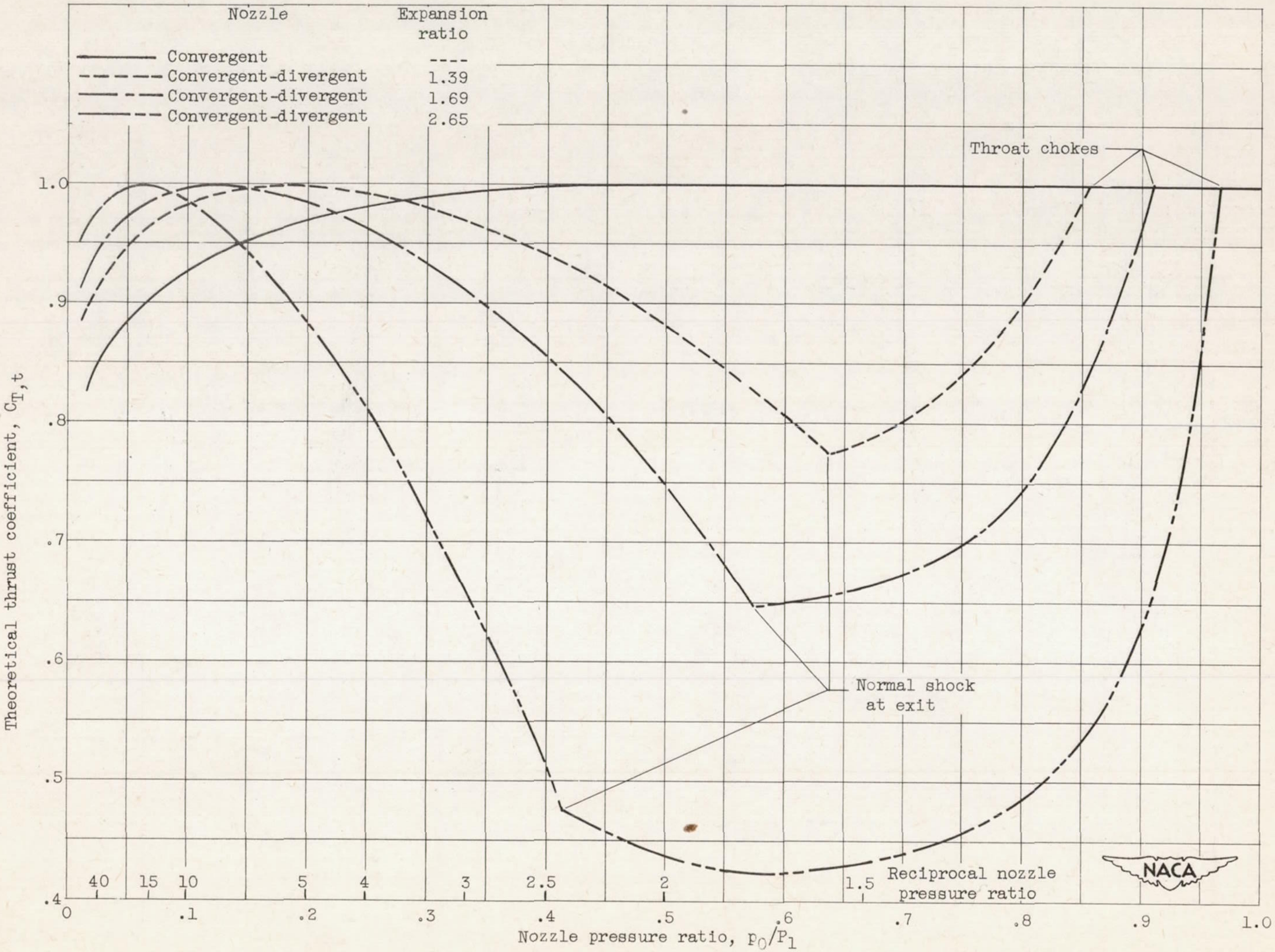

Figure 4. - Comparison of theoretical thrust coefficients for one convergent and three convergent-divergent nozzles over range of nozzle pressure ratios.

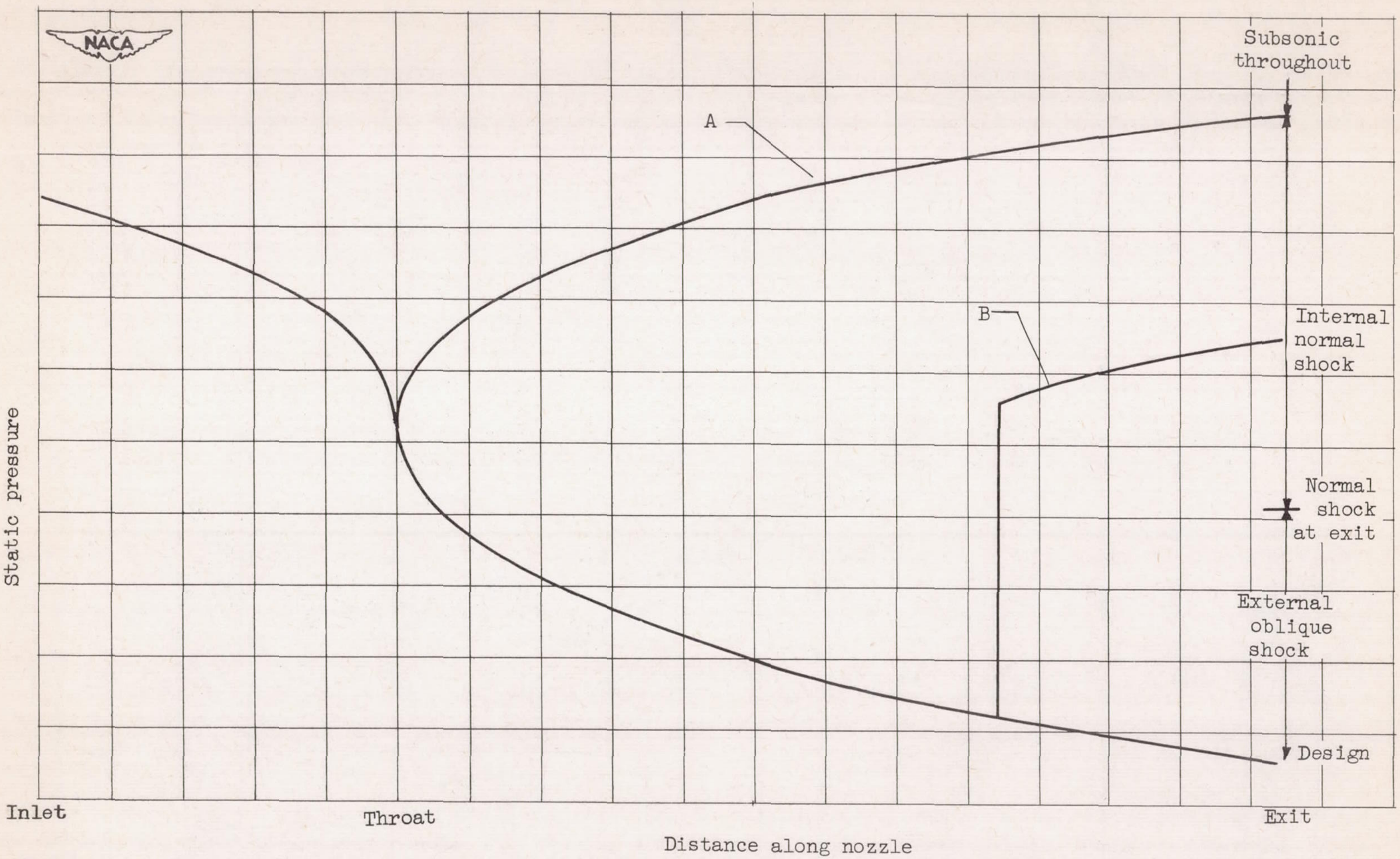

Figure 5. - Theoretical pressure distribution along convergent-divergent nozzle at various exhaust pressures. Constant nozzle-inlet pressure

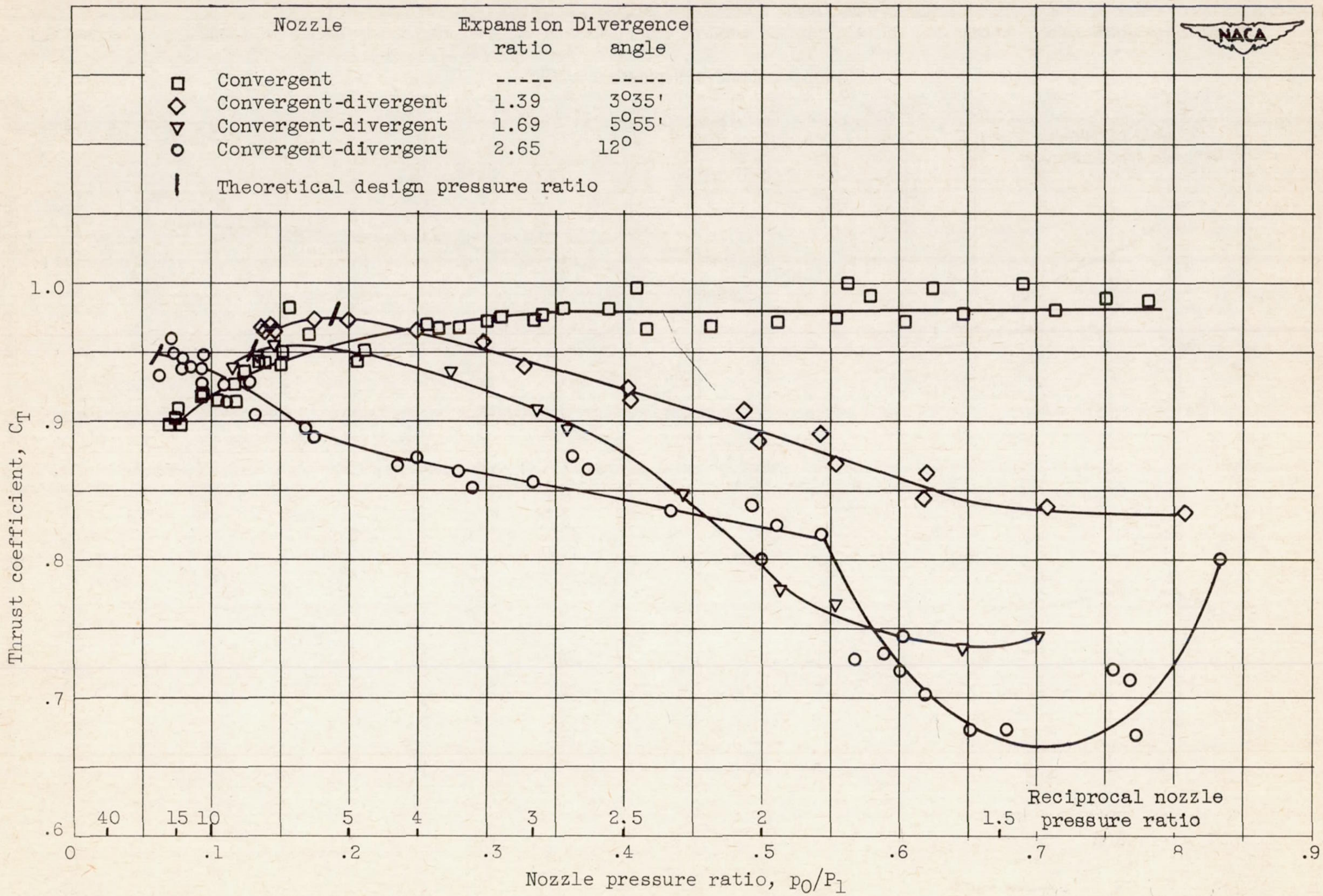

Figure 6. - Comparison of thrust coefficients for one convergent and three convergent-divergent nozzles over range of nozzle pressure ratios.

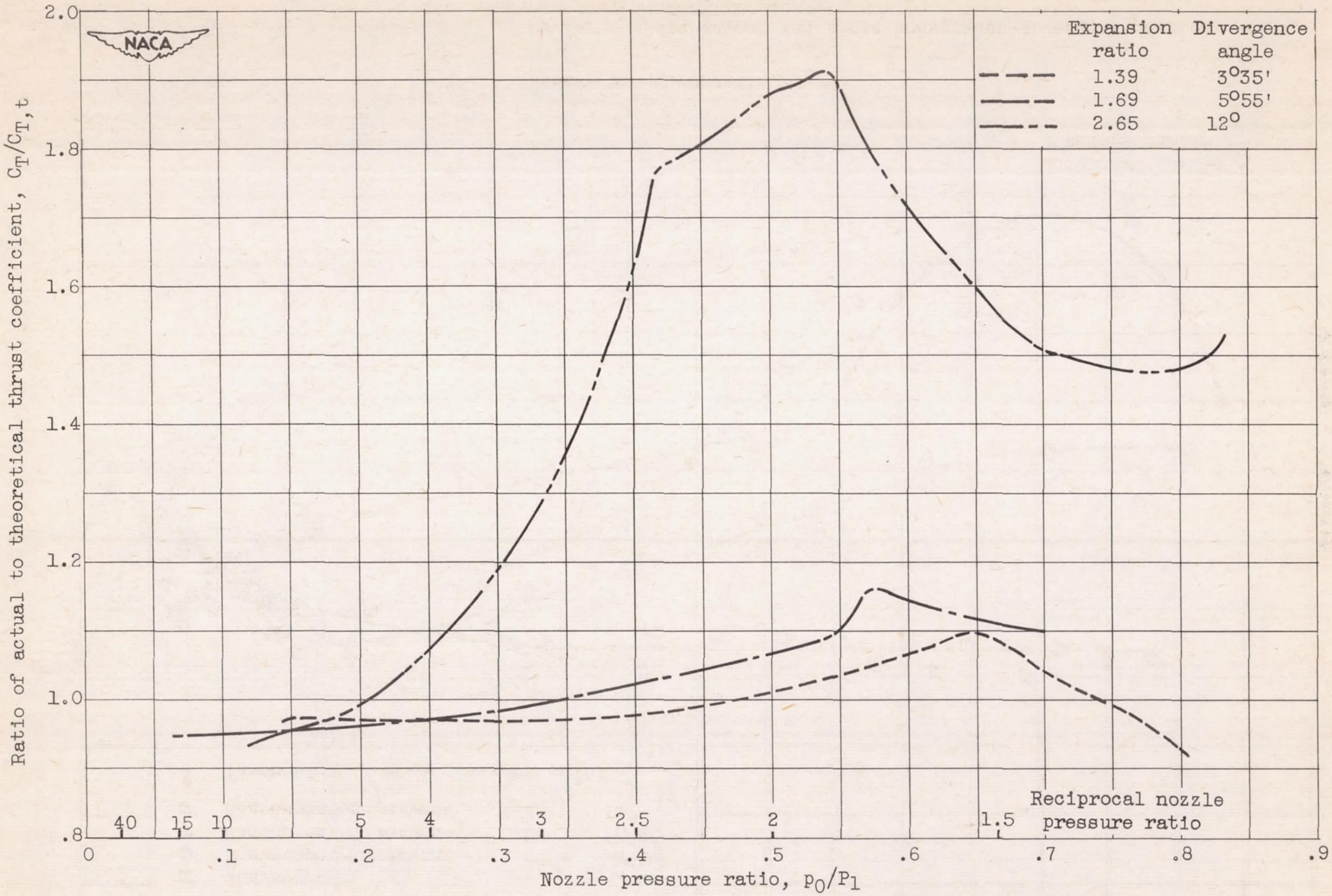

Figure 7. - Comparison of ratio of actual to theoretical thrust coefficients for three convergent-divergent nozzles with expansion ratios of 1.39, 1.69, and 2.65.

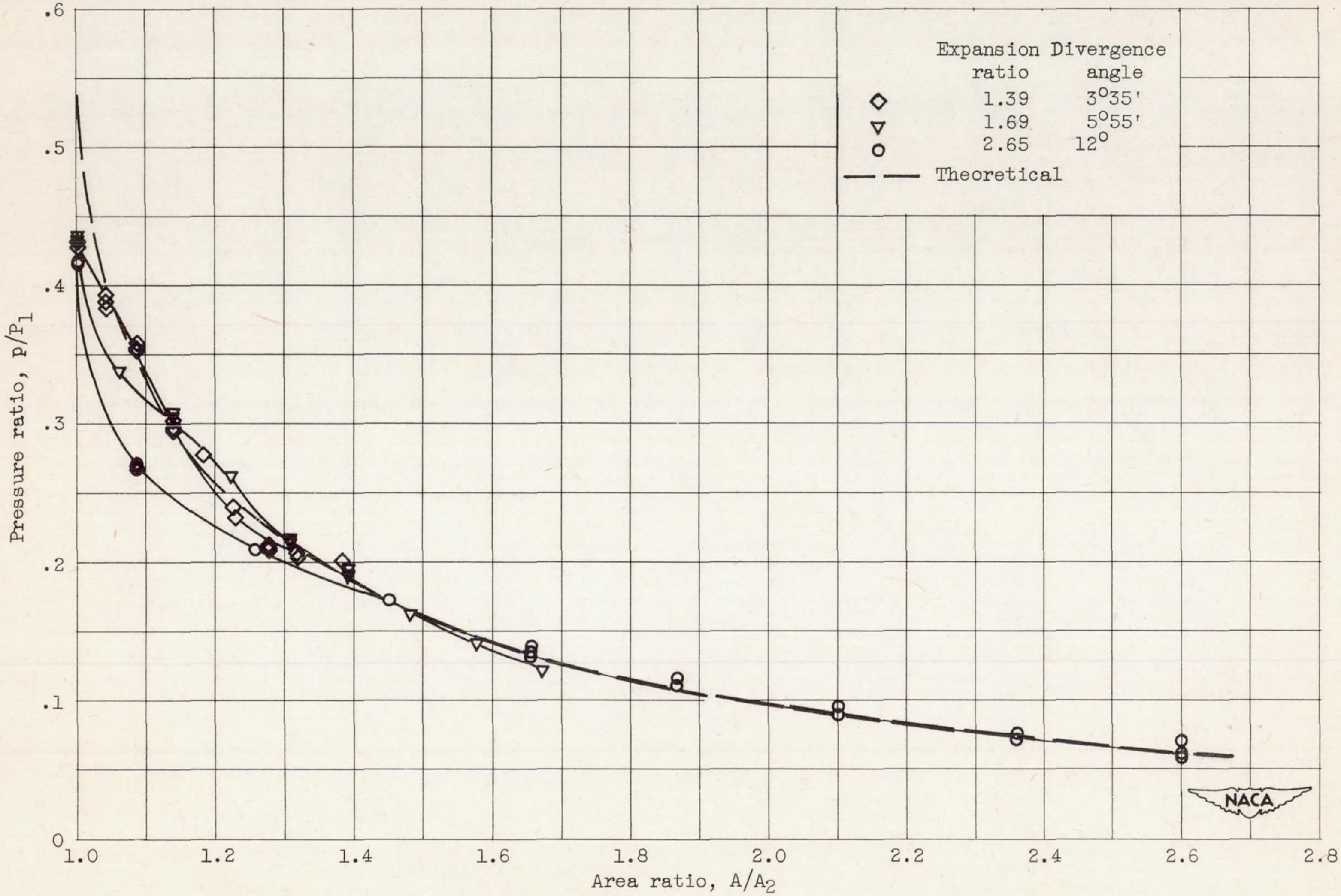

Figure 8. - Comparison of pressure distribution along diverging walls of completely expanded nozzles having expansion ratios of 1.39, 1.69, and 2.65 with theoretical expansion.

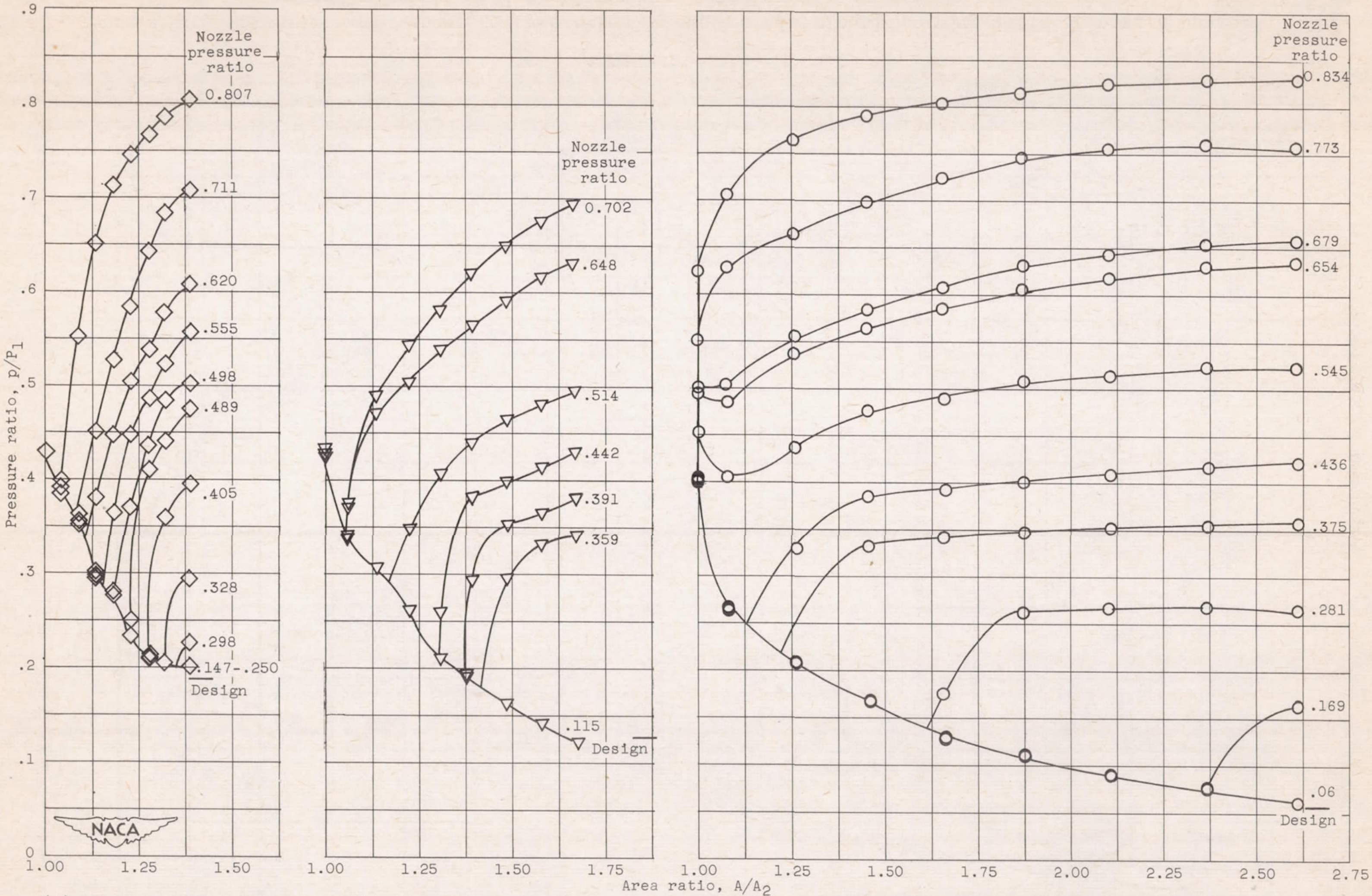

(a) Expansion ratio, 1.39.

(b) Expansion ratio, 1.69.

(c) Expansion ratio, 2.65.

Figure 9. - Pressure distribution along diverging walls of convergent-divergent nozzles at various nozzle pressure ratios.

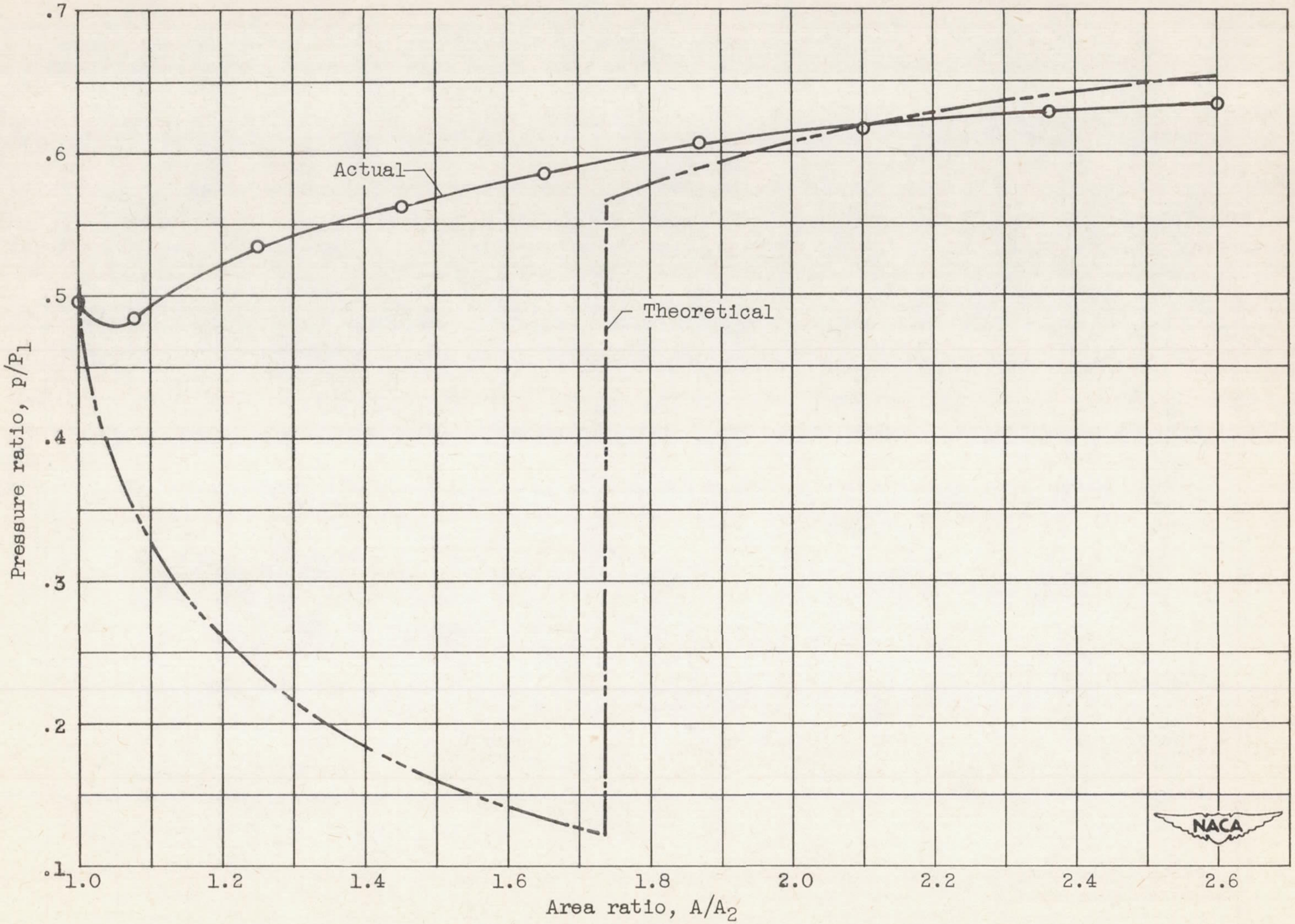

Figure 10. - Comparison of actual to theoretical pressure distribution along walls of nozzle having expansion ratio of 2.65 at nozzle pressure ratio of 0.654.

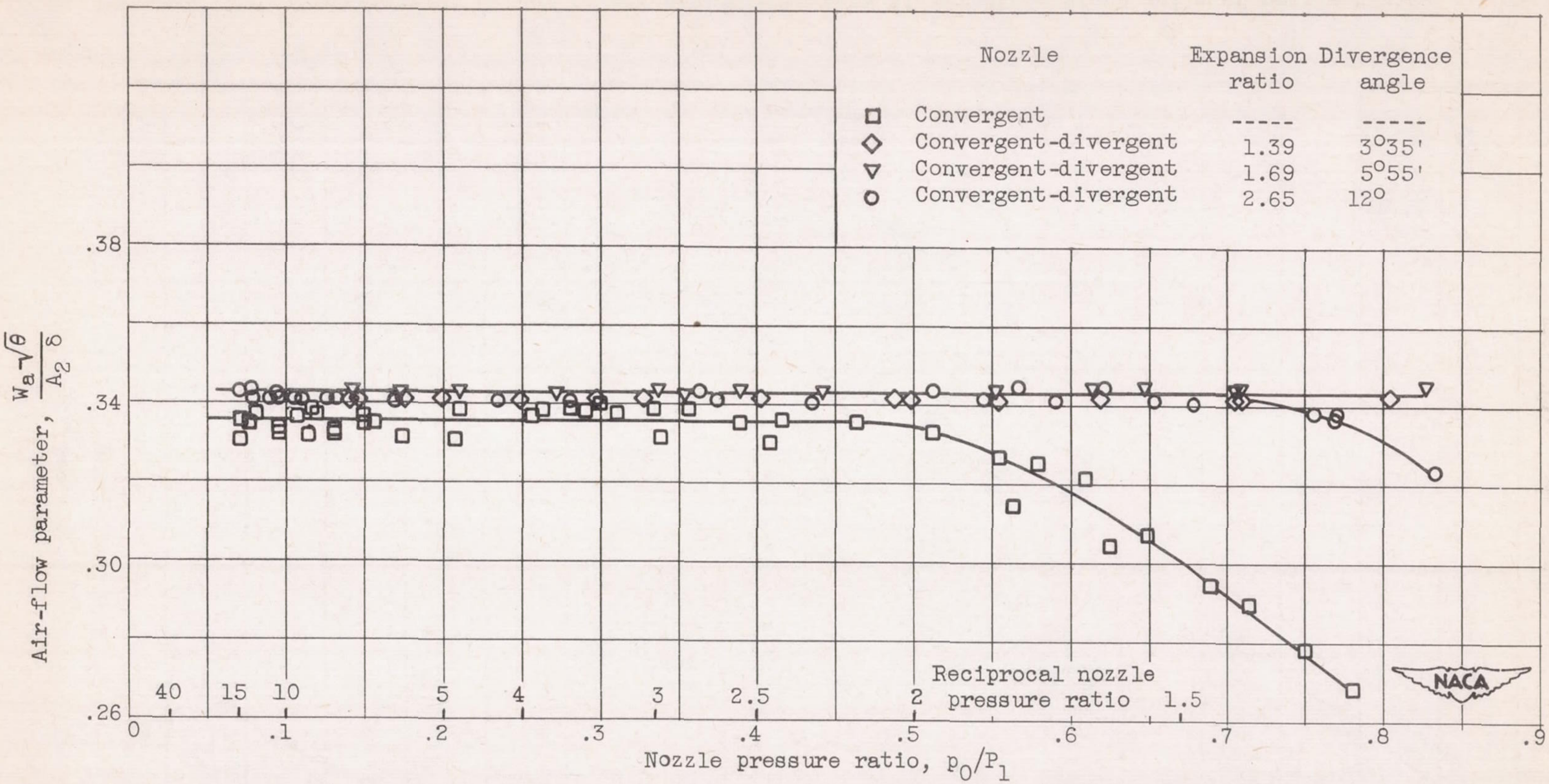

Figure 11. - Variation of air-flow parameter $W_a\sqrt{\theta}/A_2\,\delta$ with nozzle pressure ratio for convergent nozzle and convergent-divergent nozzles with expansion ratios of 1.39, 1.69, and 2.65.

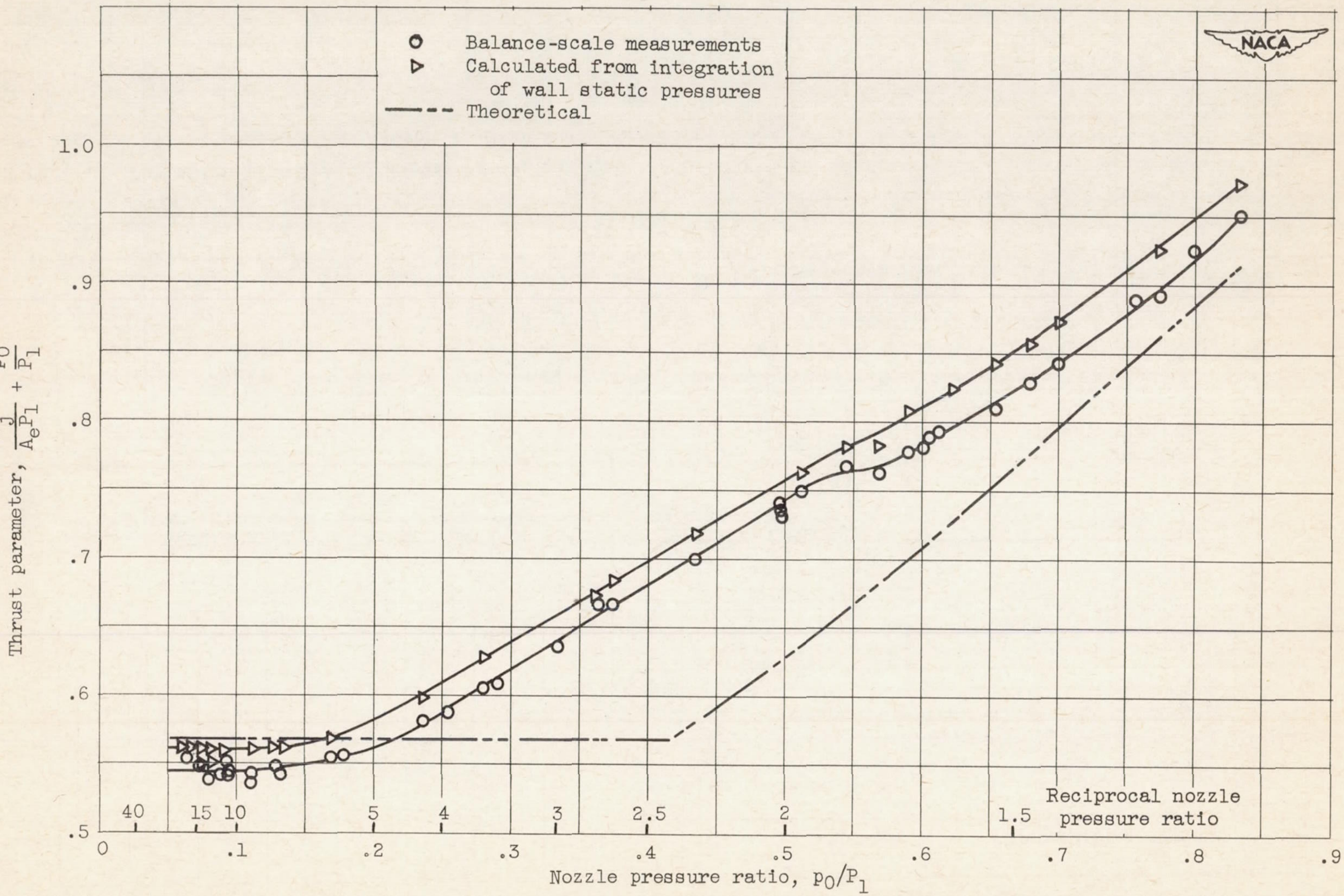

Figure 12. - Variation of thrust parameter $F_j/A_e P_1 + p_0/P_1$ with nozzle pressure ratio for nozzle having expansion ratio of 2.65.

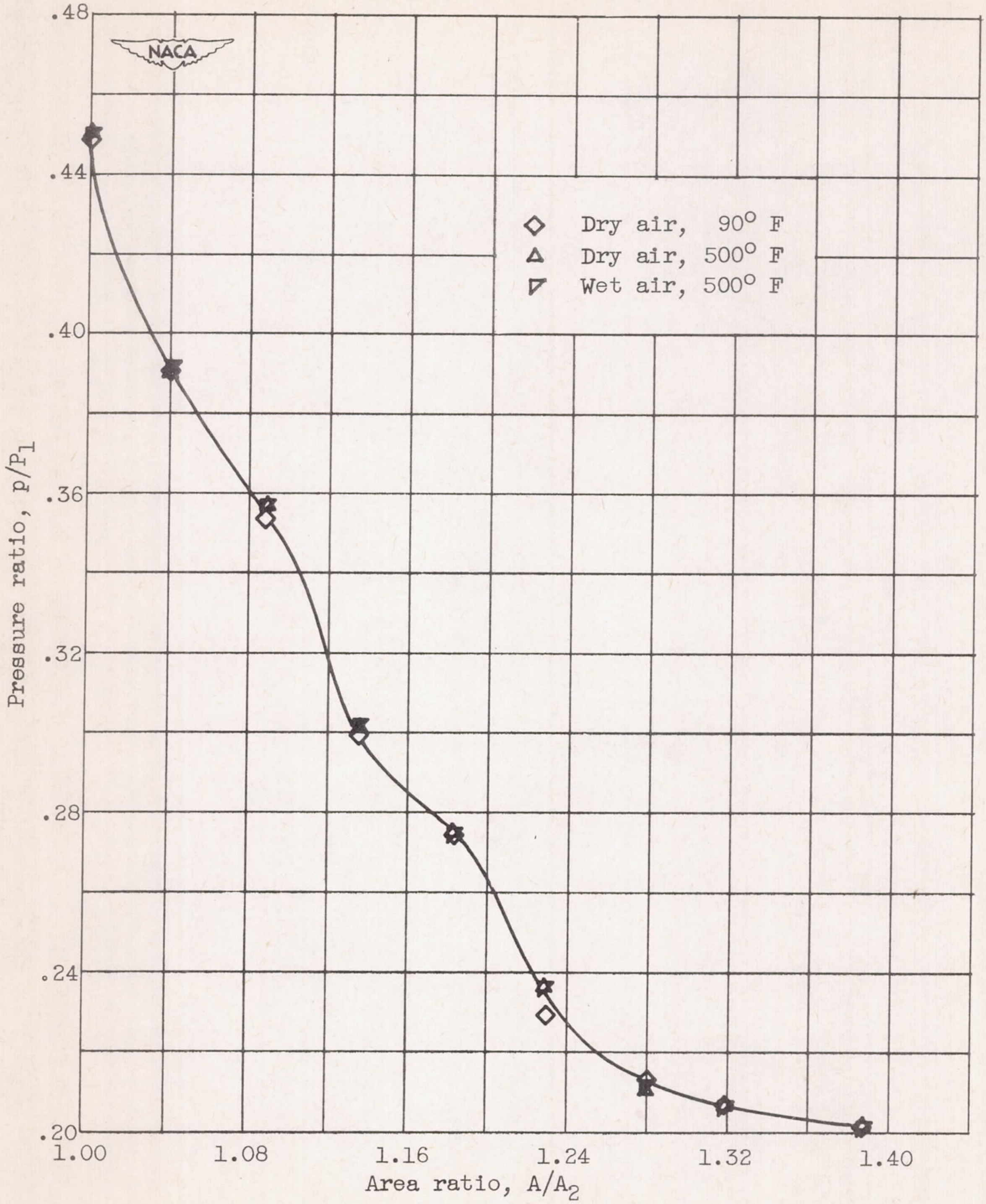

Figure 13. - Comparison of wall pressure along walls of nozzle having expansion ratio of 1.39 for hot and cold air of various moisture contents.